

Study of primordial non-Gaussianity f_{NL} and g_{NL} with the cross-correlations between the scalar-induced gravitational waves and the cosmic microwave background

Zhi-Chao Zhao,¹ Sai Wang,^{2,*} Jun-Peng Li,^{2,3} and Kazunori Kohri^{4,5,6}

¹*Department of Applied Physics, College of Science, China Agricultural University, 17 Qinghua East Road, Haidian District, Beijing 100083, China*

²*Theoretical Physics Division, Institute of High Energy Physics, Chinese Academy of Sciences, 19B Yuquan Road, Shijingshan District, Beijing 100049, China*

³*School of Physics, University of Chinese Academy of Sciences, 19A Yuquan Road, Shijingshan District, Beijing 100049, China*

⁴*Division of Science, National Astronomical Observatory of Japan (NAOJ), and SOKENDAI, 2-21-1 Osawa, Mitaka, Tokyo 181-8588, Japan*

⁵*Theory Center, IPNS, and QUP (WPI), KEK, 1-1 Oho, Tsukuba, Ibaraki 305-0801, Japan*

⁶*Kavli IPMU (WPI), UTIAS, The University of Tokyo, Kashiwa, Chiba 277-8583, Japan*

The stochastic gravitational-wave background originating from cosmic sources contains vital information about the early universe. In this work, we comprehensively study the cross-correlations between the energy-density anisotropies in scalar-induced gravitational waves (SIGWs) and the temperature anisotropies and polarization in the cosmic microwave background (CMB). In our analysis of the angular power spectra for these cross-correlations, we consider all contributions of the local-type primordial non-Gaussianity f_{NL} and g_{NL} that can lead to large anisotropies. We show that the angular power spectra are highly sensitive to primordial non-Gaussianity. Furthermore, we project the sensitivity of future gravitational-wave detectors to detect such signals and, consequently, measure the primordial non-Gaussianity.

I. INTRODUCTION

Scalar-induced gravitational waves (SIGWs) are generated nonlinearly by the linear cosmological curvature perturbations in the early universe [1–7], with their energy-density spectrum influenced by primordial non-Gaussianity [8–15]. This non-Gaussianity reflects the level of interaction of the inflaton field. Additionally, the production of SIGWs may coincide with the creation of primordial black holes (PBHs), which are considered viable candidates for dark matter [16–18]. Consequently, SIGWs serve as crucial sources of information regarding the universe’s origin and evolution during a pre-recombination era that is inaccessible with other cosmological tracers, while also potentially serving as probes of dark matter. However, observations of SIGWs may face contamination from astrophysical foregrounds, such as a stochastic gravitational-wave background from compact binary coalescences [19]. Moreover, the energy-density spectrum of SIGWs exhibits degeneracy in model parameters. To address these challenges, it is essential to introduce a comprehensive set of observables that characterize SIGWs effectively.

Studies have shown that the auto-correlations among the energy-density anisotropies in SIGWs can be a valuable tool for removing astrophysical foregrounds and addressing parameter degeneracy [20–22]. It was shown that the presence of significant anisotropies in SIGWs is contingent upon the local-type primordial non-Gaussianity [21–27]. This finding underscores the potential of the angular power spectrum as a key indicator of

inflation dynamics and a means to differentiate between various inflation models. It was also shown that the angular bispectra and trispectra of SIGWs are direct probes of primordial non-Gaussianity [23, 28]. However, the possible presence of parameter degeneracy, unknown systematics, and residual foregrounds in these auto-correlations highlights the need for additional observables to effectively address this challenge.

Cross-correlations between SIGWs and other cosmological tracers are being established to extract crucial information about the universe, getting rid of shortages of the auto-correlations. Recent analyses have investigated the cross-correlations between the energy-density anisotropies in SIGWs and the temperature anisotropies in the cosmic microwave background (CMB) [29–31]. These cross-correlations can be significant due to the shared origin of both anisotropies and the common influence of large-scale density perturbations on the propagation of gravitons and photons. Future advancements in gravitational-wave detectors and CMB experiments are poised to offer precise constraints on the non-Gaussian parameters through these cross-correlations [32–34]. Therefore, the integration of both auto- and cross-correlations would enhance our comprehension of the early universe.

In this study, we conduct a comprehensive investigation into the cross-correlations between SIGWs and the CMB. Our analysis encompasses the influence of local-type primordial non-Gaussianity, parameterized as f_{NL} and g_{NL} , on the energy density of SIGWs at both background and anisotropy levels [22]. We also examine the cross-correlations involving polarization in the CMB, besides temperature anisotropies. Furthermore, we demonstrate that the parameter degeneracy can be resolved by

* Correspondence author: wangasai@ihep.ac.cn

taking into account these cross-correlations. Through the application of the Fisher-matrix method, we evaluate the sensitivity of future gravitational-wave detectors and CMB experiments in detecting these signals and accurately measuring the non-Gaussian parameters.

The remaining of the paper is arranged as follows. By briefly summarizing the formulas for the energy-density anisotropies in SIGWs, we provide the formulas for the cross-correlations between SIGWs and the CMB in Section II. We perform the Fisher-matrix forecastings for the non-Gaussian parameter f_{NL} in Section III. We demonstrate the conclusions and discussion in Section IV.

II. CROSS-CORRELATIONS BETWEEN SIGWS AND THE CMB

In this section, we provide a brief overview of the fundamental formulas, with more comprehensive details available in Ref. [22].

A. Temperature anisotropies and polarization in the CMB

Considerable research has been dedicated to investigating temperature anisotropies and polarization in the CMB [35–37]. Photons from the early universe follow a thermal distribution resembling a blackbody spectrum. Inhomogeneities in the energy density of these relic photons result in temperature fluctuations, which are observed as temperature anisotropies in the CMB. Additionally, the presence of a quadrupole moment gives rise to polarization signals within the CMB. In this section, we present the formulas for temperature anisotropies (T) and polarization (E), excluding the consideration of B-mode polarization due to its lack of correlation with SIGWs resulting from parity constraints.

The standard practice is to express the T and E modes of the CMB in harmonic space, where the coefficients of spherical harmonics are denoted as

$$a_{X\ell m} = 4\pi(-i)^\ell \int \frac{d^3\mathbf{k}}{(2\pi)^3} e^{i\mathbf{k}\cdot\mathbf{x}_0} Y_{\ell m}^*(\hat{\mathbf{k}}) \mathcal{R}(\mathbf{k}) \Delta_{X\ell}(k, \eta_0), \quad (1)$$

where \mathcal{R} represents the primordial curvature perturbations, \mathbf{k} denotes the wavevector of these perturbations with $\hat{\mathbf{k}}$ indicating its direction, and $\Delta_{X\ell}$ corresponds to the transfer function of X (either T or E). Typically, the determination of $\Delta_{X\ell}$ involves solving the Boltzmann-Einstein equations, a task often performed using the publicly accessible CLASS¹ software [38].

The angular power spectrum of the CMB is defined as

$$\langle a_{X\ell m} a_{X'\ell' m'}^* \rangle = \delta_{\ell\ell'} \delta_{mm'} C_\ell^{\text{XX}'}, \quad (2)$$

for which we have assumed the cosmological principle. It is explicitly shown as

$$C_\ell^{\text{XX}'} = 4\pi \int d\ln k \Delta_X(k, \eta_0) \Delta_{X'}(k, \eta_0) P_L(k), \quad (3)$$

where P_L represents the dimensionless power spectrum of \mathcal{R} at large scales. For simplicity, we assume that the spectral tilt vanishes, i.e., [39, 40]

$$P_L(k) = A_L, \quad (4)$$

where A_L represents the spectral amplitude. However, it can be extended to accommodate other spectral tilts if necessary. In this study, the subscript ₀ denotes cosmological quantities in the present-day cosmos, with detailed values provided in Ref. [41].

B. Average background and the energy-density anisotropies in SIGWs

In contrast to relic photons, gravitons are intrinsically non-thermal. It is crucial to comprehend the energy-density spectrum of SIGWs before delving into the incorporation of energy-density fluctuations, which can manifest as energy-density anisotropies within SIGWs. While gravitons and relic photons travel along similar geodesics, the origins of energy-density anisotropies in SIGWs do not perfectly align with temperature anisotropies in the CMB. This discrepancy stems from the nonlinear production of SIGWs by linear cosmological curvature perturbations, necessitating the consideration of non-adiabatic initial conditions instead of the adiabatic conditions typically assumed for the CMB. Such initial conditions can lead to significant anisotropies in SIGWs in principle.

1. Average background

The energy-density (fraction) spectrum of SIGWs at the average background level has been comprehensively investigated in Refs. [22, 26, 42] by considering the local-type primordial non-Gaussianity parameters f_{NL} and g_{NL} . Additional studies on this topic are available in Refs. [21, 24, 25, 43–60]. In our approach, we utilize diagrammatic techniques to derive semi-analytical formulas for this spectrum, as detailed in Ref. [22]. Specifically, the energy-density spectrum is expressed as

$$\Omega_{\text{gw}}(\eta_i, q) = \Omega_{\text{gw}}^{(0,0)} + \Omega_{\text{gw}}^{(0,1)} + \Omega_{\text{gw}}^{(1,0)} + \Omega_{\text{gw}}^{(0,2)} + \Omega_{\text{gw}}^{(1,1)} + \Omega_{\text{gw}}^{(2,0)} + \Omega_{\text{gw}}^{(0,3)} + \Omega_{\text{gw}}^{(1,2)} + \Omega_{\text{gw}}^{(0,4)}, \quad (5)$$

where η_i signifies the production time of SIGWs, q is the gravitational-wave wavenumber, and $\Omega_{\text{gw}}^{(a,b)}$, corresponding to terms proportional to $f_{\text{NL}}^{2a} g_{\text{NL}}^b$, is detailed in Eq. (2.15) of Ref. [22]. Regarding perturbations that produce SIGWs, we consider the dimensionless power spectrum of \mathcal{R} at small scales to be

$$P_S(k) = \frac{A_S}{\sqrt{2\pi\sigma^2}} \exp\left[-\frac{\ln^2(k/k_p)}{2\sigma^2}\right], \quad (6)$$

¹ https://github.com/lesgourg/class_public

where A_S and σ represent the spectral amplitude and width, with $k_p = 2\pi f_p$ denoting the peak wavenumber with f_p being the peak frequency. Assuming $\sigma = 1$, we graphically represented $\Omega_{\text{gw}}^{(a,b)}$ as a function of q in Fig. 5 of Ref. [22] for clarity.

Ultimately, we derive the energy-density spectrum of SIGWs in the present-day universe as

$$\Omega_{\text{gw},0}(\nu) \simeq \Omega_{r,0} \Omega_{\text{gw}}(\eta_i, q), \quad (7)$$

where $\Omega_{r,0} = 4.2 \times 10^{-5} h^{-2}$, with h representing the dimensionless Hubble constant, denotes the energy-density fraction of radiation in the present-day universe, and $\nu = q/(2\pi)$ is the gravitational-wave frequency. In the above equation, we neglect contributions from effective relativistic species during the thermal evolution of the early universe, which can be reintroduced if required. Assuming $\sigma = 1$, we presented illustrations of $\Omega_{\text{gw},0}$ as a

$$\mathcal{T}_\ell = \frac{\Omega_{\text{gw},0}}{4\pi} \left\{ \left(\frac{\Omega_{\text{ng}}}{\Omega_{\text{gw}}} \right) j_\ell(k(\eta_0 - \eta_i)) + (4 - n_{\text{gw}}) T_\psi(\eta_i, k) j_\ell(k(\eta_0 - \eta_i)) \right. \\ \left. + (4 - n_{\text{gw}}) \int_{\eta_i}^{\eta_0} d\eta \left(\frac{\partial T_\phi(\eta, k)}{\partial \eta} + \frac{\partial T_\psi(\eta, k)}{\partial \eta} \right) j_\ell(k(\eta_0 - \eta)) \right\} \quad (9)$$

where the tilt of energy-density spectrum is defined as $n_{\text{gw}}(\nu) = d \ln \Omega_{\text{gw},0}(\nu) / d \ln \nu$, Ω_{ng} denotes all terms involving the couplings of long- and short-wavelength perturbations, T_ψ and T_ϕ represent the transfer functions of scalar perturbations in the comoving Newtonian gauge,

$$\Omega_{\text{ng}}(\eta_i, q) = \frac{6f_{\text{NL}}}{5} \left(4\Omega_{\text{gw}}^{(0,0)} + 3\Omega_{\text{gw}}^{(0,1)} + 2\Omega_{\text{gw}}^{(1,0)} + 2\Omega_{\text{gw}}^{(0,2)} + \Omega_{\text{gw}}^{(1,1)} + \Omega_{\text{gw}}^{(0,3)} \right) \\ + \frac{9g_{\text{NL}}}{5f_{\text{NL}}} \left(2\Omega_{\text{gw}}^{(1,0)} + 2\Omega_{\text{gw}}^{(1,1)} + 4\Omega_{\text{gw}}^{(2,0)} + 2\Omega_{\text{gw}}^{(1,2)} \right), \quad (10)$$

which aligns with Eq. (3.14) in Ref. [22]. In Eq. (9), the first term on the right-hand side represents the initial inhomogeneities, while the second and third terms correspond to the Sachs-Wolfe (SW) and integrated Sachs-Wolfe (ISW) effects [68]. The latter two effects are similar to those observed in the CMB.

It is important to highlight that the non-adiabatic initial conditions differ from the adiabatic initial conditions assumed for the CMB. When we consider a large $|f_{\text{NL}}|$ value, this distinct initial condition is responsible for the significant anisotropies in SIGWs.

In order to characterize the auto-correlations of energy-density anisotropies (G) in SIGWs, the angular power

function of ν in Fig. 6 of Ref. [22] for clarity.

2. Energy-density anisotropies

The investigation of energy-density anisotropies in SIGWs has recently been explored in Refs. [20–25, 27, 28, 30, 32, 61–66]. Specifically, we presented all contributions of f_{NL} and g_{NL} to these anisotropies in Refs. [22]. Similar to the CMB, the energy-density fluctuations of SIGWs can also be described in harmonic space. The coefficients of spherical harmonics are provided as

$$\delta_{\ell m} = 4\pi (-i)^\ell \int \frac{d^3 \mathbf{k}}{(2\pi)^3} e^{i\mathbf{k} \cdot \mathbf{x}_0} Y_{\ell m}^*(\hat{\mathbf{k}}) \mathcal{R}(\mathbf{k}) \mathcal{T}_\ell(q, k, \eta_0). \quad (8)$$

Here, the transfer function \mathcal{T}_ℓ can be derived by solving the Boltzmann-Einstein equations [23, 67]. According to Ref. [22], we explicitly represent it as

and $j_\ell(x)$ is the spherical Bessel function. In this study, we utilize energy-density fluctuations instead of energy-density contrasts. The latter are defined as the former divided by the energy density per solid angle of the average background. This convention results in a factor of $\Omega_{\text{gw},0}/(4\pi)$ in Eq. (9). We represent Ω_{ng} as follows

spectrum is defined as

$$\langle \delta_{\ell m} \delta_{\ell' m'}^* \rangle = \delta_{\ell \ell'} \delta_{m m'} C_\ell^{\text{GG}}, \quad (11)$$

leading to the following expression

$$C_\ell^{\text{GG}} = 4\pi \int d \ln k \mathcal{T}_\ell^2(q, k, \eta_0) P_L(k). \quad (12)$$

In Fig. 1, we present numerical results showcasing the auto-correlations of SIGWs, characterized by a flat angular power spectrum. We show cosmic variance (CV) in shaded regions. Here, we focus on the auto-correlations within the same frequency band of gravitational waves.

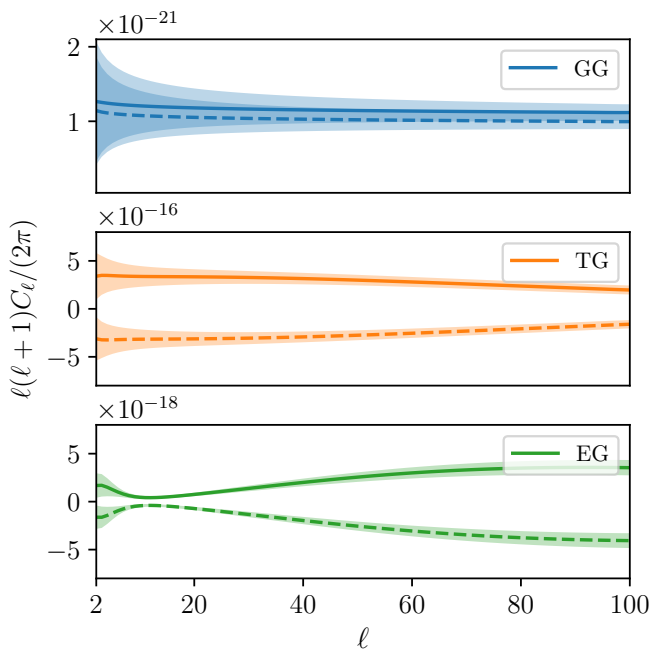


FIG. 1. The angular power spectra for the auto- and cross-correlations are shown with CV shaded. For illustration, we depict them in the frequency band of $\nu = f_p$ by assuming the model parameters $A_S = 0.02$, $\sigma = 1$, $f_{\text{NL}} = \pm 10$ (plus in solid while minus in dashed), and $g_{\text{NL}} = 20$.

However, our research methodology can be readily extended to study correlations between different frequency bands, as demonstrated in Refs. [21, 22, 30]. Based on Fig. 1, we also illustrate that the auto-correlation spectrum exhibits significant degeneracy in model parameters, as discussed in Refs. [21, 22]. In Fig. 2, we demonstrate how auto-correlations vary with different frequency bands by considering a given angular multipole moment, i.e., $\ell = 4$. Such dependence would be important to extracting vital information by performing the component separation [69, 70].

C. Cross-correlations between SIGWs and the CMB

The angular power spectrum for cross-correlations between SIGWs and the CMB is defined as

$$\frac{1}{2} \langle a_{X\ell m} \delta_{\ell' m'}^* + a_{X\ell m}^* \delta_{\ell' m'} \rangle = \delta_{\ell\ell'} \delta_{mm'} C_\ell^{\text{XG}}, \quad (13)$$

where the superscript XG indicates the cross-correlations between X-mode of the CMB and the energy-density anisotropies in SIGWs. This is explicitly expressed as

$$C_\ell^{\text{XG}} = 4\pi \int d \ln k \Delta_{X\ell}(k, \eta_0) \mathcal{T}_\ell(q, k, \eta_0) P_L(k), \quad (14)$$

which stands as one of the key outcomes of our current study. This result will be used to estimate the projected

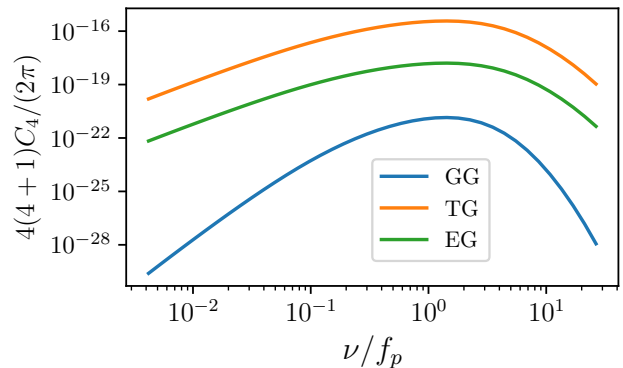


FIG. 2. We show dependence of the angular power spectra on frequency bands. For the purpose of illustration, we fix $\ell = 4$ and the model parameters $A_S = 0.02$, $\sigma = 1$, $f_{\text{NL}} = 10$, and $g_{\text{NL}} = 20$.

sensitivity of future experiments to our model parameters in the subsequent section. We also illustrate numerical results for the cross-correlations in Fig. 1 and their dependence on frequency bands in Fig. 2. Our analysis reveals that the angular power spectra for cross-correlations exhibit a nearly flat profile, with certain features being introduced by the CMB. Based on Fig. 1, we observe that the cross-correlation spectra can alleviate the degeneracy in model parameters, potentially enabling the extraction of model information. In addition, we expect that they exhibit dependence on frequency bands. Based on our analysis outlined in this section, we expect that a combination of auto- and cross-correlations would be useful to subtracting systematics and foregrounds from observations by using, e.g., component separation [69, 70]. We would leave such analysis to future works, as they are outside the scope of our current work.

We have enhanced the `GW_CLASS`² package [30] by incorporating our theoretical findings presented in this section. This modified version will be made accessible to the public on `GitHub`³ in the near future.

III. FISHER-MATRIX FORECASTINGS

In this section, utilizing the Fisher-matrix approach⁴ [72], we investigate the precision of measuring model parameters by detecting the cross-correlations between SIGWs and the CMB using upcoming gravitational-wave detection. For the purpose of illustration, our focus is

² https://github.com/lesgourg/class_public/tree/GW_CLASS

³ <https://github.com>

⁴ Ref. [71] introduced a Bayesian approach, which could be applied to our current study in principle. Nevertheless, for illustrative purposes, we anticipate that the Fisher-matrix approach will be adequate for our theoretical analysis.

solely on the non-linear parameter f_{NL} , and thereby let $g_{\text{NL}} = 0$. Nevertheless, our research methodology can be readily extended to encompass other model parameters as required. Throughout this work, we do not consider potential sources of astrophysical foregrounds, which are left to be studied by future works.

The signal-to-noise ratio (SNR) for a combination of auto- and cross-correlations is defined as

$$\text{SNR}^2 = \sum_{\ell=2}^{\ell_{\text{max}}} \mathbf{C}^T \mathbf{C}^{-1} \mathbf{C}, \quad (15)$$

where we define $\mathbf{C} = (C_{\ell}^{\text{GG}}, C_{\ell}^{\text{TG}}, C_{\ell}^{\text{EG}})^T$, and the covariance matrix is represented as⁵

$$\mathbb{C} = \begin{pmatrix} \sigma_{\ell}^{\text{GG-GG}^2} & \sigma_{\ell}^{\text{GG-TG}^2} & \sigma_{\ell}^{\text{GG-EG}^2} \\ \sigma_{\ell}^{\text{GG-TG}^2} & \sigma_{\ell}^{\text{TG-TG}^2} & \sigma_{\ell}^{\text{TG-EG}^2} \\ \sigma_{\ell}^{\text{GG-EG}^2} & \sigma_{\ell}^{\text{TG-EG}^2} & \sigma_{\ell}^{\text{EG-EG}^2} \end{pmatrix}. \quad (17)$$

Our analysis includes the noise characteristics N_{ℓ} of gravitational-wave detectors⁶, while considering only CV for the CMB since the noise in future CMB experiments could potentially be dominated by CV. When ignoring N_{ℓ} , we obtain an inevitable uncertainty due to CV.

To evaluate the precision of measuring model parameters, we utilize the Fisher matrix F , defined as

$$F_{ij} = \sum_{\ell=2}^{\ell_{\text{max}}} \frac{\partial \mathbf{C}^T}{\partial p_i} \mathbb{C}^{-1} \frac{\partial \mathbf{C}}{\partial p_j}, \quad (18)$$

where $\partial \mathbf{C} / \partial p_i$ denotes the derivative of each element of \mathbf{C} with respect to the model parameter p_i , and ℓ_{max} represents the maximum value of angular multipole moments

⁵ Elements of \mathbb{C} are specifically given as

$$\sigma_{\ell}^{\text{GG-GG}^2} = \frac{2}{2\ell+1} (C_{\ell}^{\text{GG}} + N_{\ell})^2, \quad (16a)$$

$$\sigma_{\ell}^{\text{GG-TG}^2} = \frac{2}{2\ell+1} [(C_{\ell}^{\text{GG}} + N_{\ell}) C_{\ell}^{\text{TG}}], \quad (16b)$$

$$\sigma_{\ell}^{\text{GG-EG}^2} = \frac{2}{2\ell+1} [(C_{\ell}^{\text{GG}} + N_{\ell}) C_{\ell}^{\text{EG}}], \quad (16c)$$

$$\sigma_{\ell}^{\text{TG-TG}^2} = \frac{1}{2\ell+1} [(C_{\ell}^{\text{TG}})^2 + C_{\ell}^{\text{TT}} (C_{\ell}^{\text{GG}} + N_{\ell})], \quad (16d)$$

$$\sigma_{\ell}^{\text{TG-EG}^2} = \frac{1}{2\ell+1} [C_{\ell}^{\text{TE}} (C_{\ell}^{\text{GG}} + N_{\ell}) + C_{\ell}^{\text{TG}} C_{\ell}^{\text{EG}}], \quad (16e)$$

$$\sigma_{\ell}^{\text{EG-EG}^2} = \frac{1}{2\ell+1} [(C_{\ell}^{\text{EG}})^2 + C_{\ell}^{\text{EE}} (C_{\ell}^{\text{GG}} + N_{\ell})]. \quad (16f)$$

⁶ We use the North American Nanohertz Observatory for Gravitational Waves (NANOGrav) [73], Laser Interferometer Space Antenna (LISA) [74, 75], Big Bang Observer (BBO) [76, 77], Deci-hertz Interferometer Gravitational wave Observatory (DECIGO) [78, 79], and a network of Einstein Telescope (ET) [80] and Cosmic Explorer (CE) [81]. We utilize the noise from the most sensitive frequency band for each detector [82, 83]. We depict them in Fig. 3 to compare with the specified signal. Similar methodologies can be applied to analyze other detectors.

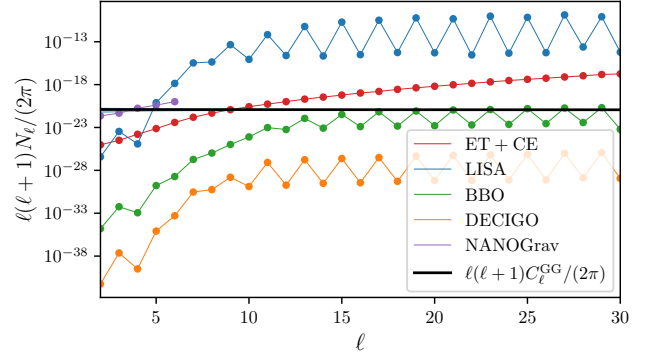


FIG. 3. Comparison between the signal and the optimal sensitivity of detectors. The noise level of NANOGrav is illustrated as the lowest in the lower panel of Fig. 4 in Ref. [82], while the noise levels of other detectors are depicted in Fig. 7 of Ref. [83]. In our analysis, we consider a set of model parameters $f_{\text{NL}} = 10$, $g_{\text{NL}} = 0$, $A_S = 0.02$, $\sigma = 1$, and $f_p = f_*$ with f_* being the frequency associated with the optimal sensitivity. For the signal, we utilize the specified auto-correlated angular power spectrum at $\nu = f_p$.

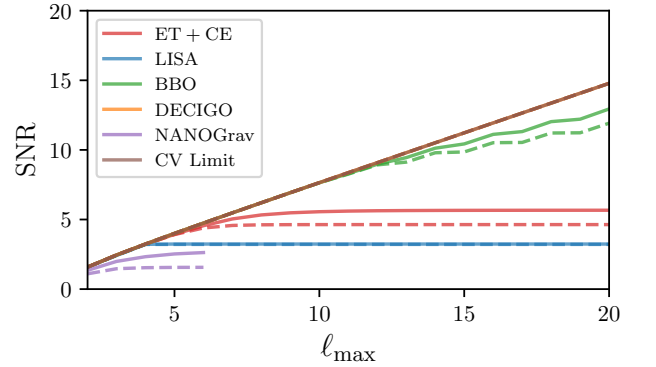


FIG. 4. The SNRs are depicted for the detection of auto-correlations (dashed curves) and both auto- and cross-correlations (solid curves) using future gravitational-wave detectors. We adopt the same set of model parameters as those in Fig. 3. For comparison, we include the CV limits. It is worth noting that the curves corresponding to DECIGO perfectly align with the CV limits.

that are relevant for a given detector. For the sake of clarity, we concentrate on a single parameter, specifically $p_1 = f_{\text{NL}}$. The 1σ uncertainty of f_{NL} is determined by the Cramér-Rao bound, i.e.,

$$\sigma_{f_{\text{NL}}} = \sqrt{(F^{-1})_{11}}, \quad (19)$$

which provides a rough estimate of the measurement precision. This level of analysis is adequate for our theoretical investigation.

To assess the performance of detectors in measuring auto- and cross-correlations, we present the SNRs as a

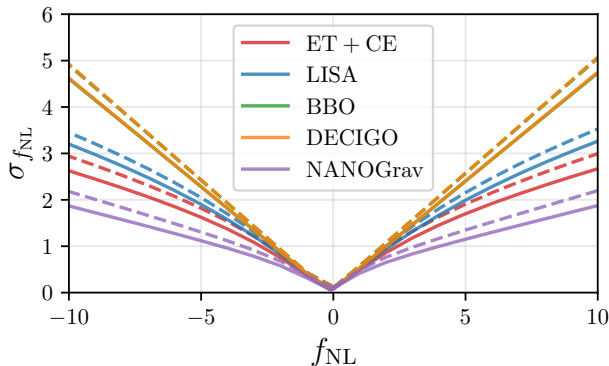


FIG. 5. The uncertainties in f_{NL} are assessed by measuring the auto-correlations (dashed curves) and both auto- and cross-correlations (solid curves) using prospective gravitational-wave detectors. We use $\ell_{\text{max}} = 6$ for NANOGrav while $\ell_{\text{max}} = 30$ for others. For each f_{NL} value, we calculate A_S setting $\text{SNR} = 1$ in the auto-correlation-only case, while assuming $g_{\text{NL}} = 0$, $\sigma = 1$, and $f_p = f_*$.

function of ℓ_{max} in Fig. 4. In this analysis, we assume $f_{\text{NL}} = 10$, $g_{\text{NL}} = 0$, $A_S = 0.02$, $\sigma = 1$, and $f_p = f_*$, where f_* represents the frequency associated with the optimal sensitivity of detectors. We examine two scenarios: one focusing solely on auto-correlations and the other involving a combination of auto- and cross-correlations. Our findings reveal that the inclusion of cross-correlations consistently improves the SNR compared to the auto-correlation-only scenario. Nevertheless, the SNR for both cases potentially reaches a saturation point with increasing ℓ_{max} due to the limitations in detectors' angular resolution. Additionally, we present the CV limits for comparison. For the specified signal, DECIGO can achieve the CV limits as its noise level is significantly lower than CV. Conversely, other detectors are able to approach the CV limits only at the lowest angular multipole moments.

To assess the precision of parameter estimation for the model, we analyze the uncertainties in f_{NL} measured by the detectors under consideration in Fig. 5. We use $\ell_{\text{max}} = 6$ for NANOGrav while $\ell_{\text{max}} = 30$ for others. We examine the same two cases as depicted in Fig. 4, but for each f_{NL} value, we determine A_S by setting $\text{SNR} = 1$ in the auto-correlation-only case. For the specified signal, we observe that the combination of auto- and cross-correlations yields reduced uncertainties in estimating this parameter compared to the case focusing solely on auto-correlations. By increasing the SNR, these uncertainties can be proportionally reduced.

IV. CONCLUSIONS AND DISCUSSION

Our study focused on exploring the cross-correlation between the energy-density anisotropies in SIGWs and the temperature anisotropies and polarization in the

CMB. We derived the expressions for the corresponding angular power spectra and integrated them as template banks into our customized version of `GW_CLASS`. It is worth noting that our analysis accounted for all contributions stemming from the local-type primordial non-Gaussian parameters f_{NL} and g_{NL} , which have the potential to significantly alter the existing findings in the literature. We suggested that the distinct dependencies of the angular power spectra on model parameters could prove instrumental in resolving degeneracies within these parameters. Furthermore, we determined the projected sensitivity of multi-band gravitational-wave detectors and CMB experiments in detecting these signals and precisely measuring our model parameters, especially those related to primordial non-Gaussianity. We anticipate that the combination of auto- and cross-correlations will enrich our understanding of the early universe.

The energy-density anisotropies in SIGWs may have origins partially attributed to the SW and ISW effects, akin to those observed in the CMB but with subtle distinctions. Gravitons were generated before the radiation-matter equality epoch and traversed longer distances compared to the last scattering of photons. In contrast to the CMB, SIGWs are additionally influenced by contributions from effective relativistic species and the early ISW effect predating the recombination era. In our present investigation, we considered these effects by utilizing the modified version of `GW_CLASS`. Our findings indicate that the anisotropies in SIGWs stemming from these effects are at a level of approximately $\sim 10^{-4}$, which is comparable to the $\sim 10^{-5}$ level observed in the CMB [41]. Furthermore, it is important to acknowledge that the SW and ISW effects are independent of specific models and are inherent in the observations.

The initial inhomogeneities in SIGWs are inherent to the system and contingent on the specific production mechanism, thus encapsulating information about the underlying model. In our current study, we consider the non-adiabatic initial conditions that have been extensively explored in our previous works. Unlike the CMB, the significant anisotropies in SIGWs can be attributed to these initial conditions, particularly in the presence of local-type primordial non-Gaussianity. In such scenarios, it is anticipated that short-wavelength modes will interact with long-wavelength modes, with the former nonlinearly generating SIGWs. Consequently, the spatial distribution of energy density in SIGWs is influenced by the modulation induced by the latter.

We derived the angular power spectra for the auto- and cross-correlations, revealing their strong dependence on the level of primordial non-Gaussianity. On the one hand, we may be capable of differentiating SIGWs from astrophysical foregrounds by examining the distinctive features present in their angular power spectra. Specifically, the angular power spectra of SIGWs exhibit characteristic scalings of $\ell(\ell + 1)C_\ell \sim \ell^0$, in contrast to those of SGWB originating from binary black holes which roughly follow $\ell(\ell + 1)C_\ell \sim \ell^1$ [67, 84–94]. This dispar-

ity in scaling suggests the potential to distinguish between these two signal components based on their angular power spectrum characteristics [20, 95, 96]. On the other hand, our findings indicated that combining the cross-correlation spectra can alleviate the parameter degeneracy observed in the auto-correlation spectrum. This outcome has the potential to distinguish between various models of inflation. Therefore, our investigation may pave the way for novel approaches to measure non-Gaussian parameters and, consequently, delve into the origins and early evolution of the universe.

We delved deeper into exploring the anticipated sensitivity of forthcoming multi-band gravitational-wave detectors in measuring model parameters, specifically focusing on the non-Gaussian parameter f_{NL} . Our analysis revealed that the combined consideration of both auto- and cross-correlated angular power spectra could effectively enhance precision in parameter measurements. Furthermore, we identified the inherent limitations on the precision of these measurements stemming from CV.

Our research methodology can be extended to investigate cross-correlations between SIGWs (or other sources of SGWB) and other cosmological probes such as large-scale structures (LSS), hydrogen 21 cm lines, etc. However, we defer these investigations to future works as they fall outside the scope of our present research.

ACKNOWLEDGMENTS

S.W. and J.P.L. are supported by the National Key R&D Program of China No. 2023YFC2206403 and the National Natural Science Foundation of China (Grant No. 12175243). Z.C.Z. is supported by the National Key Research and Development Program of China Grant No. 2021YFC2203001. K.K. is supported by KAKENHI Grant Nos. JP22H05270, JP23KF0289, JP24H01825, JP24K07027. This work is supported by the High-performance Computing Platform of China Agricultural University.

-
- [1] K.N. Ananda, C. Clarkson and D. Wands, *The Cosmological gravitational wave background from primordial density perturbations*, *Phys. Rev. D* **75** (2007) 123518 [[gr-qc/0612013](#)].
 - [2] D. Baumann, P.J. Steinhardt, K. Takahashi and K. Ichiki, *Gravitational Wave Spectrum Induced by Primordial Scalar Perturbations*, *Phys. Rev. D* **76** (2007) 084019 [[hep-th/0703290](#)].
 - [3] J.R. Espinosa, D. Racco and A. Riotto, *A Cosmological Signature of the SM Higgs Instability: Gravitational Waves*, *JCAP* **09** (2018) 012 [[1804.07732](#)].
 - [4] K. Kohri and T. Terada, *Semianalytic calculation of gravitational wave spectrum nonlinearly induced from primordial curvature perturbations*, *Phys. Rev. D* **97** (2018) 123532 [[1804.08577](#)].
 - [5] S. Mollerach, D. Harari and S. Matarrese, *CMB polarization from secondary vector and tensor modes*, *Phys. Rev. D* **69** (2004) 063002 [[astro-ph/0310711](#)].
 - [6] H. Assadullahi and D. Wands, *Constraints on primordial density perturbations from induced gravitational waves*, *Phys. Rev. D* **81** (2010) 023527 [[0907.4073](#)].
 - [7] G. Domènech, *Scalar Induced Gravitational Waves Review*, *Universe* **7** (2021) 398 [[2109.01398](#)].
 - [8] J.M. Maldacena, *Non-Gaussian features of primordial fluctuations in single field inflationary models*, *JHEP* **05** (2003) 013 [[astro-ph/0210603](#)].
 - [9] N. Bartolo, E. Komatsu, S. Matarrese and A. Riotto, *Non-Gaussianity from inflation: Theory and observations*, *Phys. Rept.* **402** (2004) 103 [[astro-ph/0406398](#)].
 - [10] T.J. Allen, B. Grinstein and M.B. Wise, *Nongaussian Density Perturbations in Inflationary Cosmologies*, *Phys. Lett. B* **197** (1987) 66.
 - [11] N. Bartolo, S. Matarrese and A. Riotto, *Nongaussianity from inflation*, *Phys. Rev. D* **65** (2002) 103505 [[hep-ph/0112261](#)].
 - [12] V. Acquaviva, N. Bartolo, S. Matarrese and A. Riotto, *Second order cosmological perturbations from inflation*, *Nucl. Phys. B* **667** (2003) 119 [[astro-ph/0209156](#)].
 - [13] F. Bernardeau and J.-P. Uzan, *NonGaussianity in multifield inflation*, *Phys. Rev. D* **66** (2002) 103506 [[hep-ph/0207295](#)].
 - [14] X. Chen, M.-x. Huang, S. Kachru and G. Shiu, *Observational signatures and non-Gaussianities of general single field inflation*, *JCAP* **01** (2007) 002 [[hep-th/0605045](#)].
 - [15] C.T. Byrnes and K.-Y. Choi, *Review of local non-Gaussianity from multi-field inflation*, *Adv. Astron.* **2010** (2010) 724525 [[1002.3110](#)].
 - [16] B. Carr and F. Kuhnel, *Primordial Black Holes as Dark Matter: Recent Developments*, *Ann. Rev. Nucl. Part. Sci.* **70** (2020) 355 [[2006.02838](#)].
 - [17] B. Carr, K. Kohri, Y. Sendouda and J. Yokoyama, *Constraints on primordial black holes*, *Rept. Prog. Phys.* **84** (2021) 116902 [[2002.12778](#)].
 - [18] B. Carr, S. Clesse, J. Garcia-Bellido, M. Hawkins and F. Kuhnel, *Observational evidence for primordial black holes: A positivist perspective*, *Phys. Rept.* **1054** (2024) 1 [[2306.03903](#)].
 - [19] T. Regimbau, *The astrophysical gravitational wave stochastic background*, *Res. Astron. Astrophys.* **11** (2011) 369 [[1101.2762](#)].
 - [20] LISA COSMOLOGY WORKING GROUP collaboration, *Probing anisotropies of the Stochastic Gravitational Wave Background with LISA*, *JCAP* **11** (2022) 009 [[2201.08782](#)].
 - [21] J.-P. Li, S. Wang, Z.-C. Zhao and K. Kohri, *Primordial non-Gaussianity f_{NL} and anisotropies in scalar-induced gravitational waves*, *JCAP* **10** (2023) 056 [[2305.19950](#)].
 - [22] J.-P. Li, S. Wang, Z.-C. Zhao and K. Kohri, *Complete analysis of the background and anisotropies of scalar-induced gravitational waves: primordial non-Gaussianity f_{NL} and g_{NL} considered*, *JCAP* **06**

- (2024) 039 [2309.07792].
- [23] N. Bartolo, D. Bertacca, V. De Luca, G. Franciolini, S. Matarrese, M. Peloso et al., *Gravitational wave anisotropies from primordial black holes*, *JCAP* **02** (2020) 028 [1909.12619].
- [24] S. Wang, Z.-C. Zhao, J.-P. Li and Q.-H. Zhu, *Implications of pulsar timing array data for scalar-induced gravitational waves and primordial black holes: Primordial non-Gaussianity fNL considered*, *Phys. Rev. Res.* **6** (2024) L012060 [2307.00572].
- [25] Y.-H. Yu and S. Wang, *Anisotropies in scalar-induced gravitational-wave background from inflaton-curvaton mixed scenario with sound speed resonance*, *Phys. Rev. D* **109** (2024) 083501 [2310.14606].
- [26] J.A. Ruiz and J. Rey, *Gravitational waves in ultra-slow-roll and their anisotropy at two loops*, **2410.09014**.
- [27] J. Rey, *A consistency relation for induced gravitational wave anisotropies*, **2411.08873**.
- [28] J.-P. Li, S. Wang, Z.-C. Zhao and K. Kohri, *Angular bispectrum and trispectrum of scalar-induced gravitational waves: all contributions from primordial non-Gaussianity f_{NL} and g_{NL}* , *JCAP* **05** (2024) 109 [2403.00238].
- [29] E. Dimastrogiovanni, M. Fasiello, A. Malhotra and G. Tasinato, *Enhancing gravitational wave anisotropies with peaked scalar sources*, *JCAP* **01** (2023) 018 [2205.05644].
- [30] F. Schulze, L. Valbusa Dall'Armi, J. Lesgourgues, A. Ricciardone, N. Bartolo, D. Bertacca et al., *GW_CLASS: Cosmological Gravitational Wave Background in the cosmic linear anisotropy solving system*, *JCAP* **10** (2023) 025 [2305.01602].
- [31] R.-G. Cai, S.-J. Wang, Z.-Y. Yuwen and X.-X. Zeng, *Anisotropies of cosmological gravitational wave backgrounds in non-flat spacetime*, **2410.17721**.
- [32] A. Malhotra, E. Dimastrogiovanni, M. Fasiello and M. Shiraiishi, *Cross-correlations as a Diagnostic Tool for Primordial Gravitational Waves*, *JCAP* **03** (2021) 088 [2012.03498].
- [33] G. Perna, A. Ricciardone, D. Bertacca and S. Matarrese, *Non-Gaussianity from the cross-correlation of the astrophysical Gravitational Wave Background and the Cosmic Microwave Background*, *JCAP* **10** (2023) 014 [2302.08429].
- [34] P. Adshead, N. Afshordi, E. Dimastrogiovanni, M. Fasiello, E.A. Lim and G. Tasinato, *Multimessenger cosmology: Correlating cosmic microwave background and stochastic gravitational wave background measurements*, *Phys. Rev. D* **103** (2021) 023532 [2004.06619].
- [35] U. Seljak and M. Zaldarriaga, *A Line of sight integration approach to cosmic microwave background anisotropies*, *Astrophys. J.* **469** (1996) 437 [astro-ph/9603033].
- [36] M. Zaldarriaga and U. Seljak, *An all sky analysis of polarization in the microwave background*, *Phys. Rev. D* **55** (1997) 1830 [astro-ph/9609170].
- [37] M. Kamionkowski, A. Kosowsky and A. Stebbins, *Statistics of cosmic microwave background polarization*, *Phys. Rev. D* **55** (1997) 7368 [astro-ph/9611125].
- [38] D. Blas, J. Lesgourgues and T. Tram, *The cosmic linear anisotropy solving system (class). part ii: Approximation schemes*, *Journal of Cosmology and Astroparticle Physics* **2011** (2011) 034–034.
- [39] J.-Q. Jiang and Y.-S. Piao, *Toward early dark energy and $n_s=1$ with Planck, ACT, and SPT observations*, *Phys. Rev. D* **105** (2022) 103514 [2202.13379].
- [40] G. Ye, J.-Q. Jiang and Y.-S. Piao, *Toward inflation with $n_s=1$ in light of the Hubble tension and implications for primordial gravitational waves*, *Phys. Rev. D* **106** (2022) 103528 [2205.02478].
- [41] PLANCK collaboration, *Planck 2018 results. VI. Cosmological parameters*, *Astron. Astrophys.* **641** (2020) A6 [1807.06209].
- [42] C. Yuan, D.-S. Meng and Q.-G. Huang, *Full analysis of the scalar-induced gravitational waves for the curvature perturbation with local-type non-Gaussianities*, *JCAP* **12** (2023) 036 [2308.07155].
- [43] T. Nakama, J. Silk and M. Kamionkowski, *Stochastic gravitational waves associated with the formation of primordial black holes*, *Phys. Rev. D* **95** (2017) 043511 [1612.06264].
- [44] J. Garcia-Bellido, M. Peloso and C. Unal, *Gravitational Wave signatures of inflationary models from Primordial Black Hole Dark Matter*, *JCAP* **09** (2017) 013 [1707.02441].
- [45] P. Adshead, K.D. Lozanov and Z.J. Weiner, *Non-Gaussianity and the induced gravitational wave background*, *JCAP* **10** (2021) 080 [2105.01659].
- [46] H.V. Ragavendra, *Accounting for scalar non-Gaussianity in secondary gravitational waves*, *Phys. Rev. D* **105** (2022) 063533 [2108.04193].
- [47] H.V. Ragavendra, P. Saha, L. Sriramkumar and J. Silk, *Primordial black holes and secondary gravitational waves from ultraslow roll and punctuated inflation*, *Phys. Rev. D* **103** (2021) 083510 [2008.12202].
- [48] S. Garcia-Saenz, L. Pinol, S. Renaux-Petel and D. Werth, *No-go theorem for scalar-trispectrum-induced gravitational waves*, *JCAP* **03** (2023) 057 [2207.14267].
- [49] K.T. Abe, R. Inui, Y. Tada and S. Yokoyama, *Primordial black holes and gravitational waves induced by exponential-tailed perturbations*, *JCAP* **05** (2023) 044 [2209.13891].
- [50] R.-g. Cai, S. Pi and M. Sasaki, *Gravitational Waves Induced by non-Gaussian Scalar Perturbations*, *Phys. Rev. Lett.* **122** (2019) 201101 [1810.11000].
- [51] C. Unal, *Imprints of Primordial Non-Gaussianity on Gravitational Wave Spectrum*, *Phys. Rev. D* **99** (2019) 041301 [1811.09151].
- [52] V. Atal and G. Domènech, *Probing non-Gaussianities with the high frequency tail of induced gravitational waves*, *JCAP* **06** (2021) 001 [2103.01056].
- [53] C. Yuan and Q.-G. Huang, *Gravitational waves induced by the local-type non-Gaussian curvature perturbations*, *Phys. Lett. B* **821** (2021) 136606 [2007.10686].
- [54] F. Zhang, *Primordial black holes and scalar induced gravitational waves from the E model with a Gauss-Bonnet term*, *Phys. Rev. D* **105** (2022) 063539 [2112.10516].
- [55] J. Lin, S. Gao, Y. Gong, Y. Lu, Z. Wang and F. Zhang, *Primordial black holes and scalar induced gravitational waves from Higgs inflation with noncanonical kinetic term*, *Phys. Rev. D* **107** (2023) 043517 [2111.01362].
- [56] L.-Y. Chen, H. Yu and P. Wu, *Primordial non-Gaussianity in inflation with gravitationally enhanced friction*, *Phys. Rev. D* **106** (2022) 063537 [2210.05201].

- [57] Z. Chang, Y.-T. Kuang, D. Wu, J.-Z. Zhou and Q.-H. Zhu, *New constraints on primordial non-Gaussianity from missing two-loop contributions of scalar induced gravitational waves*, *Phys. Rev. D* **109** (2024) L041303 [2311.05102].
- [58] R.-G. Cai, S. Pi, S.-J. Wang and X.-Y. Yang, *Pulsar Timing Array Constraints on the Induced Gravitational Waves*, *JCAP* **10** (2019) 059 [1907.06372].
- [59] G. Perna, C. Testini, A. Ricciardone and S. Matarrese, *Fully non-Gaussian Scalar-Induced Gravitational Waves*, *JCAP* **05** (2024) 086 [2403.06962].
- [60] X.-X. Zeng, R.-G. Cai and S.-J. Wang, *Multiple peaks in gravitational waves induced from primordial curvature perturbations with non-Gaussianity*, *JCAP* **10** (2024) 045 [2406.05034].
- [61] L. Valbusa Dall'Armi, A. Ricciardone, N. Bartolo, D. Bertacca and S. Matarrese, *Imprint of relativistic particles on the anisotropies of the stochastic gravitational-wave background*, *Phys. Rev. D* **103** (2021) 023522 [2007.01215].
- [62] E. Dimastrogiovanni, M. Fasiello, A. Malhotra, P.D. Meerburg and G. Orlando, *Testing the early universe with anisotropies of the gravitational wave background*, *JCAP* **02** (2022) 040 [2109.03077].
- [63] LISA COSMOLOGY WORKING GROUP collaboration, *Cosmology with the Laser Interferometer Space Antenna*, *Living Rev. Rel.* **26** (2023) 5 [2204.05434].
- [64] C. Ünal, E.D. Kovetz and S.P. Patil, *Multimessenger probes of inflationary fluctuations and primordial black holes*, *Phys. Rev. D* **103** (2021) 063519 [2008.11184].
- [65] A. Malhotra, E. Dimastrogiovanni, G. Domènech, M. Fasiello and G. Tasinato, *New universal property of cosmological gravitational wave anisotropies*, *Phys. Rev. D* **107** (2023) 103502 [2212.10316].
- [66] L. Valbusa Dall'Armi, A. Mierna, S. Matarrese and A. Ricciardone, *Adiabatic or Non-Adiabatic? Unraveling the Nature of Initial Conditions in the Cosmological Gravitational Wave Background*, **2307.11043**.
- [67] C.R. Contaldi, *Anisotropies of Gravitational Wave Backgrounds: A Line Of Sight Approach*, *Phys. Lett. B* **771** (2017) 9 [1609.08168].
- [68] R.K. Sachs and A.M. Wolfe, *Perturbations of a cosmological model and angular variations of the microwave background*, *Astrophys. J.* **147** (1967) 73.
- [69] S. Kuwahara and L. Tsukada, *Applicability of multi-component study on Bayesian searches for targeted anisotropic stochastic gravitational-wave background*, **2411.19761**.
- [70] Z.-C. Liang, Z.-Y. Li, E.-K. Li, J.-d. Zhang and Y.-M. Hu, *Unveiling a multi-component stochastic gravitational-wave background with the TianQin + LISA network*, **2409.00778**.
- [71] C. Tian, R. Ding and X.-X. Kou, *Estimating the gravitational wave background anisotropy: a Bayesian approach boosted by cross-correlation angular power spectrum*, **2412.01219**.
- [72] A. Ly, M. Marsman, J. Verhagen, R. Grasman and E.-J. Wagenmakers, *A tutorial on fisher information*, 2017.
- [73] F. Jenet, L.S. Finn, J. Lazio, A. Lommen, M. McLaughlin, I. Stairs et al., *The north american nanohertz observatory for gravitational waves*, 2009.
- [74] J. Baker et al., *The Laser Interferometer Space Antenna: Unveiling the Millihertz Gravitational Wave Sky*, **1907.06482**.
- [75] T.L. Smith, T.L. Smith, R.R. Caldwell and R. Caldwell, *LISA for Cosmologists: Calculating the Signal-to-Noise Ratio for Stochastic and Deterministic Sources*, *Phys. Rev. D* **100** (2019) 104055 [1908.00546].
- [76] J. Crowder and N.J. Cornish, *Beyond LISA: Exploring future gravitational wave missions*, *Phys. Rev. D* **72** (2005) 083005 [gr-qc/0506015].
- [77] T.L. Smith and R. Caldwell, *Sensitivity to a Frequency-Dependent Circular Polarization in an Isotropic Stochastic Gravitational Wave Background*, *Phys. Rev. D* **95** (2017) 044036 [1609.05901].
- [78] N. Seto, S. Kawamura and T. Nakamura, *Possibility of direct measurement of the acceleration of the universe using 0.1-Hz band laser interferometer gravitational wave antenna in space*, *Phys. Rev. Lett.* **87** (2001) 221103 [astro-ph/0108011].
- [79] S. Kawamura et al., *Current status of space gravitational wave antenna DECIGO and B-DECIGO*, *PTEP* **2021** (2021) 05A105 [2006.13545].
- [80] S. Hild, S. Chelkowski and A. Freise, *Pushing towards the ET sensitivity using 'conventional' technology*, **0810.0604**.
- [81] D. Reitze et al., *Cosmic Explorer: The U.S. Contribution to Gravitational-Wave Astronomy beyond LIGO*, *Bull. Am. Astron. Soc.* **51** (2019) 035 [1907.04833].
- [82] N. Pol, S.R. Taylor and J.D. Romano, *Forecasting Pulsar Timing Array Sensitivity to Anisotropy in the Stochastic Gravitational Wave Background*, *Astrophys. J.* **940** (2022) 173 [2206.09936].
- [83] M. Braglia and S. Kuroyanagi, *Probing prerecombination physics by the cross-correlation of stochastic gravitational waves and CMB anisotropies*, *Phys. Rev. D* **104** (2021) 123547 [2106.03786].
- [84] G. Cusin, I. Dvorkin, C. Pitrou and J.-P. Uzan, *First predictions of the angular power spectrum of the astrophysical gravitational wave background*, *Phys. Rev. Lett.* **120** (2018) 231101 [1803.03236].
- [85] G. Cusin, C. Pitrou and J.-P. Uzan, *Anisotropy of the astrophysical gravitational wave background: Analytic expression of the angular power spectrum and correlation with cosmological observations*, *Phys. Rev. D* **96** (2017) 103019 [1704.06184].
- [86] G. Cusin, I. Dvorkin, C. Pitrou and J.-P. Uzan, *Stochastic gravitational wave background anisotropies in the mHz band: astrophysical dependencies*, *Mon. Not. Roy. Astron. Soc.* **493** (2020) L1 [1904.07757].
- [87] G. Cusin, I. Dvorkin, C. Pitrou and J.-P. Uzan, *Properties of the stochastic astrophysical gravitational wave background: astrophysical sources dependencies*, *Phys. Rev. D* **100** (2019) 063004 [1904.07797].
- [88] A.C. Jenkins, R. O'Shaughnessy, M. Sakellariadou and D. Wysocki, *Anisotropies in the astrophysical gravitational-wave background: The impact of black hole distributions*, *Phys. Rev. Lett.* **122** (2019) 111101 [1810.13435].
- [89] A.C. Jenkins, M. Sakellariadou, T. Regimbau and E. Slezak, *Anisotropies in the astrophysical gravitational-wave background: Predictions for the detection of compact binaries by LIGO and Virgo*, *Phys. Rev. D* **98** (2018) 063501 [1806.01718].
- [90] A.C. Jenkins, J.D. Romano and M. Sakellariadou, *Estimating the angular power spectrum of the*

- gravitational-wave background in the presence of shot noise, *Phys. Rev. D* **100** (2019) 083501 [1907.06642].
- [91] S. Wang, V. Vardanyan and K. Kohri, *Probing primordial black holes with anisotropies in stochastic gravitational-wave background*, *Phys. Rev. D* **106** (2022) 123511 [2107.01935].
- [92] S. Mukherjee and J. Silk, *Time-dependence of the astrophysical stochastic gravitational wave background*, *Mon. Not. Roy. Astron. Soc.* **491** (2020) 4690 [1912.07657].
- [93] S.S. Bavera, G. Franciolini, G. Cusin, A. Riotto, M. Zevin and T. Fragos, *Stochastic gravitational-wave background as a tool for investigating multi-channel astrophysical and primordial black-hole mergers*, *Astron. Astrophys.* **660** (2022) A26 [2109.05836].
- [94] N. Bellomo, D. Bertacca, A.C. Jenkins, S. Matarrese, A. Raccanelli, T. Regimbau et al., *CLASS_GWB: robust modeling of the astrophysical gravitational wave background anisotropies*, *JCAP* **06** (2022) 030 [2110.15059].
- [95] Y. Cui, S. Kumar, R. Sundrum and Y. Tsai, *Unraveling cosmological anisotropies within stochastic gravitational wave backgrounds*, *JCAP* **10** (2023) 064 [2307.10360].
- [96] Z.-C. Zhao and S. Wang, *Measuring the anisotropies in astrophysical and cosmological gravitational-wave backgrounds with Taiji and LISA networks*, *Sci. China Phys. Mech. Astron.* **67** (2024) 120411 [2407.09380].